

Synthesis Characterization Morphology and Thermal Study of CuO Metal Oxide by Using Liquid-Liquid Interface Reaction

Jyothilaxmi¹, H.V. Vijayanand^{2*}, Dhondiba V³, and A. ⁴Venkataraman

¹ PDA College of Engineering, Kalaburagi

² Government College (Autonomous), Kalaburagi.

³ Government Women's First Grade College, Kalaburagi.

⁴Gulbarga University Kalaburgi-585103.

Abstract

Nano sized CuO particles were prepared by organic-aqueous layer by the reaction of ferric Acetylacetonate and copper acetylacetonate in toluene with sodium hydroxide in aqueous solution. The nanocrystals of CuO are formed at the interface of the organic-aqueous layer have been confirmed by X-ray diffraction (XRD). Infra-red spectroscopy (IR) scanning electron micrograph (SEM) and transmission electron micrograph (TEM) techniques, thermal XRD and SEM/TEM studies reveals that the products are monophasic copper oxide having nanosized particles. The SEM describes about the morphology and TEM express about the shape and size and thermal study express about the strength of the nano-particles of CuO.

Key words: Liquid-Liquid, Chemical synthesis, metal oxides and Characterization.

1. Introduction:

• Nanomaterials:

The Solid State Chemistry has become part of the formal training program in chemistry [1]. Being one of the frontiers of chemistry, it has a tremendous future and certainly demands the active involvement of many more chemists. The present time, Solid State Chemistry is mainly concerned with the development of new methods of synthesis, new ways of identifying, characterizing materials and describing their structure with desired and controllable properties.

Transition metal oxides constitute the most fascinating class of materials, exhibiting a variety of structures and properties [2]. The metal-oxygen bond can vary anywhere between highly ionic to covalent or metallic. The unusual properties of transition metal oxides are clearly due to the unique nature of the outer d-electrons. The phenomenal range of electronic and magnetic properties, exhibited by transition metal oxides is noteworthy. Thus the electrical resistivity in oxide materials spans the wide range of 10^{-10} to $10^{20}\Omega$ cm. We have oxides with metallic properties (e.g. RuO_2 , RuO_3) at the other. There are also oxides that transverse both, these regimes with changes in temperature, pressure or

* Author for Correspondence: v_havanoor@rediffmail.com

composition (e.g. V_2O_3 , $\text{La}_{1-x}\text{Sr}_x\text{VO}_3$). Interesting electronic properties also arise from charge density wave (e.g. $\text{K}_{0.3}\text{MoO}_3$), charge ordering (e.g. Fe_3O_4) and defect ordering (e.g. $\text{Ca}_2\text{Mn}_2\text{O}_5$, $\text{Ca}_2\text{Fe}_2\text{O}_5$). Oxides with diverse magnetic properties anywhere from ferromagnetism (e.g. CrO_2 , $\text{La}_{0.5}\text{Sr}_{0.5}\text{MnO}_3$) to antiferromagnetism (e.g. NiO , LaCrO_3 , $\alpha\text{-Fe}_2\text{O}_3$) are known. Many oxides possess switchable orientation states as in ferroelectric (e.g. BaTiO_3 , KNbO_3) and ferroelastic [e.g. $\text{Gd}_2(\text{MoO}_4)_3$] materials. Then, there are a variety of oxide bronzes showing a gamut of property [3].

Maghemite ($\gamma\text{-Fe}_2\text{O}_3$) nanoparticles have attracted great attention in recent years because of their wide application in the areas of ferrofluids, high information storage¹² [4], magnetic resonance imaging (MRI), [5-7] labeling and sorting of cells [8] and separation of biochemical products [9,10]. Maghemite is a ferromagnetic oxide that has been already widely used as magnetic recording materials. Due to the chemical stability, biocompatibility and the heating ability of maghemite nanoparticles can be also used for ferrofluids hyperthermia (MFH) in tumor treatment [11].

Most of above mentioned applications require the nanoparticles to be chemically stable and uniform in development of synthetic procedures to iron oxide nanoparticles, such as template methods [12, 13], micro-wave and γ -irradiation methods [14], sonolysis [15], microemulsion methods [16] thermal decomposition method [17,18], solvothermal method [19], Langmuir-Blodgett techniques³⁰ [20], microwave technique [21] etc. Many of these methods involved in the synthesis of metal oxides are tedious, some of them time consuming with many reaction steps and often suffer from the difficulty of tedious post-treatment procedures and reproducibility and also the formation of agglomerates cannot be ruled out. In contrast to the other methods, interfaces between immiscible liquids is a one step process enabling synthesis of nanocrystal arrays at the liquid-liquid interface and this method is known to be ideal for assembling of colloidal particles [22, 23]. Brust et al. [24] used immiscible water-organic solvent mixtures in the presence of phase-transferring reagents to prepare metal organosols. Rao et al. [25] have carried out an extensive experiments on nanocrystalline films obtained at the interface and found them to be essentially single crystalline in nature. Experiments by Rao et al., also revealed that it was indeed possible to prepare nanocrystals of metals [26-27] and other materials at the liquid-liquid interface through the reaction of an organometallic precursor taken in the organic layer with an appropriate reagent in the aqueous layer.

In the present investigation, we have made use of this novel synthetic route employing two immiscible liquids such as toluene and water, with the metal organic precursor (ferric acetylacetonate) in the organic layer and the hydrolyzing agent in the aqueous layer. Similarly, the synthesis of CuO metal oxide a suitable organic derivative metal taken in the organic layer reacts at the interface with the appropriate reagent present in the organic layer. Importance was given to the synthesis of CuO in this article.

Liquid-Liquid interface method is a one-step synthesis enabling synthesis of nanocrystal arrays at the liquid-liquid interface under ambient conditions. The diameters range of the

nanoneedle form 2-8 nm and the lengths range from 30-100 nm. These nanoneedles are distributed irregularly throughout the grid. Vary fine particles of 8-10 nm are also besides the needles on careful observations. The TEM results suggest that the sample is light crystallinity in nature.

2. Materials and Methods:

Copper sulphate (CuSO_4), acetylacetonate, Sodium hydroxide (NaOH) and other chemicals used were AR grade. These solvents well purified and double distilled water were used.

2.1 Synthesis of CuO metal oxide using Liquid-Liquid Interfacial Method:

Ultra-fine films of inorganic materials have been prepared by a variety of methods. Physical methods such as thermal evaporation, laser ablation, vacuum sputtering and molecular beam epitaxy basically involved the evaporation of the reactants using high energy followed by condensation on a substrate yielding thin films of materials, Chemical methods such as chemical vapor deposition (CVD) and electro deposition generally employed in milder conditions. Thin films of nanocrystals have been prepared employing the Langmuir-Blodgett [LB] technique in the recent past and other materials have been prepared at the air water interface by the LB technique. The features and properties of a thin film generally depend on the nature of the substrate as well as on the technique and conditions employed for generating the film. Thus, thin films of inorganic materials are often polycrystalline or possess island structures. Since it is not always easy to obtain robust films of nanocrystals through self-assembly, it would be of great advantage to devise a suitable method of obtaining ultra-thin films which are continuous over a wide area and are single crystalline in nature. In this context, the use of the liquid-liquid interface for generating nanocrystalline films of metals, metal-chalcogenides, and metal oxides is significant between immiscible liquids and are known to be ideal for assembling of colloidal particles.

Liquid-Liquid interface method is a one-step synthesis enabling synthesis of nanocrystal arrays at the liquid-liquid interface under ambient conditions. The method involves the reaction of an organometallic compound dissolved in the organic layer with reducing, sulfiding, or an oxidizing agent in the aqueous layer. The material formed at the interface is an ultra-thin nano crystalline film, consisting of closely packed nanocrystals. A careful examination has shown that the materials formed at the interface is an ultra-thin nanocrystalline film consisting of closely packed metal/metal oxide nanocrystals coated with the organic species present at the interface. The other advantages of this invention are as follows: mild reaction conditions, easy to operate, short process period and easy to industrialize.

Hence the objectives of the present work are to prepare and characterize one of the widely used ceramic oxides, viz., $\gamma\text{-Fe}_2\text{O}_3$ and CuO , NiO , CoO etc, some metal oxides using cost-effective and relatively at simple room temperature liquid-liquid interface method.

The method used for the synthesis of nanoparticles was liquid-liquid interfacial method. The method is discussed in the present article.

1) Preparation of precursors:

- **Preparation of copper acetyl acetate complex:**

Dissolved about 3 gm of Copper sulphate (CuSO_4) in 20 ml of water. In another beaker 2.6 ml of acetylacetonate is taken and treated with 0.1 N Sodium hydroxide (NaOH) solution drop by drop with constant stirring till the oily appearance on the acetyl acetone disappears. Add a drop or more, Dissolve the sodium salt of acetyl acetone in about 10 ml of water (H_2O). Add the solution to the CuSO_4 solution with constant stirring until blue precipitate of Cu(II) acetyl acetone complex is formed and allow it, to stand for about 30 minutes. Then filter and dry it. The colors of obtained precursor are as shown in Fig. 2.

- **Synthesis off nanosized CuO metal oxide:**

The synthesis of these nano particles was carried out by employing liquid-liquid interfacial reaction method. Proper desired grams of above prepared copper acetylacetonate complex was weighed and added to 100 ml pure toluene solution. After complete dissolution, the solution is added to a beaker containing 100 ml of 4N sodium hydroxide (NaOH) solution. The reaction mixture is allowed to stand for 40 hours. The reaction mixture slowly organic layer turns pale blue color and the interface turn to blue color forming a film as shown in the fig.2. The film was removed slowly and washed several times with double distilled water then with ethanol to remove inorganic and organic impurities and later sonicated After 2 days there is a formation of solid substance at the junction of these two layers, which is separated by decanting and filtering. After separation it is dried over 50°C temperature. The color of respective metal oxide is as shown in Fig. (4).

3. Characterization techniques:

- **X-ray diffraction:**

Since the discovery in 1912 by Von Laue, X-ray diffraction has provided a wealth of important information to science and industry. For much that is to be known about the arrangement and the spacing of atoms in crystalline materials has been directly deduced from diffraction studies. These studies proved to be of immense importance in understanding the physical properties of metals, metal oxides and other solids non-destructively. The application of X-ray diffraction methods to chemical analysis is primarily in the identification of compounds present from their diffraction patterns and determination of the relative concentration by the intensities of pattern lines.

W.L. Bragg showed from the below equation that the X-rays reflected from a lattice plane and the effect associated with it could be derived by the equation.

$$n\lambda = 2d \sin\theta$$

Where 'n' is an integer (the "order"), λ the wavelength of the X-rays, d the inter-planar spacing and θ is the angle of incidence of the X-ray beam on the lattice plane.

In crystalline powder, the tiny crystals are oriented at random. If an X-ray beam strikes such a powder, many planes will be so oriented, that Bragg's law is simultaneously satisfied and an X-ray diffraction pattern is obtained. To be certain that all possible planes are exposed to the X-ray beam, the specimen is usually rotated by an angle θ on its own axis during exposure. Most

of the X-ray beam will pass directly through the sample and diffracted beams, which are collected by a detector (scintillation counter). It is rotated by 2θ the output of which is processed and then fed into an automatic recorder. The result is a chart which gives a record of counts per second (proportional and diffracted beam intensity) versus diffraction angle 2θ .

The X-ray powder diffraction patterns of the solid sample or films were obtained using JEOL JDX-8P X-ray diffractometer. The target used was Cu K_α or Co K_α radiation. The X-ray generator was operated at 30 kV and 20 mA. The scanning range, $2\theta/\theta$ was selected. The scanning speed = 1° or 4° min^{-1} , chart speed = 20 mm min^{-1} were employed for precise lattice parameter determination. High purity silicon powder was used as an internal standard.

The d spacing of cubic ferrites, for a given set of planes (hkl) is given by:

$$d_{hkl} = \frac{n\lambda}{2 \sin \theta}$$

Where λ = wave length of the X-ray radiation in Å.

n = order of reflection and

θ = glancing angle of incidence.

- **Determination of average crystallite sizes from X-ray line broadening**

The average crystallite size (D) from X-ray line broadening has been calculated using the Scherer equation [28-29]

$$D = \frac{0.9 \lambda}{\beta_{1/2} \cos \theta}$$

Where λ is the wavelength of the X-ray beam; $\beta_{1/2}$ is the angular width at the half-maximum intensity and θ is the Bragg angle. The instrumental broadening was collected using quartz as internal standard.

- **Density evaluation from X-ray data**

The X-ray density of the sample have been computed from the values of lattice parameters for cubic system, using the formula C

$$d = \frac{8 M}{N a^3}$$

Where 8 represents the number of molecules in a unit cell of a spinel lattice

M = Molecular weight of the ferrite sample

N = Avogadro's number, and

A = lattice parameter of the ferrite

The lattice constant a for cubic was calculated using equation

$$d = \frac{a}{(h^2 + k^2 + l^2)^{1/2}}$$

- **Infrared spectroscopy:**

Infrared spectroscopy has widely been used for the identification of the functional groups in organic compounds because of the fact that their spectra are generally complex and provide numerous peaks that can be used for comparison purpose. In fact the infrared absorption spectrum of an organic compound is a fingerprint of its functional groups.

An infrared spectrum for metal oxides has been reported to some extent in literature. The main reason for this study includes Characterisation of metal-oxygen frequencies and detecting the presence of water along with impurities if any, identification of M-O peaks characterizes a particular class of compounds (e.g., two peaks one at 450 and other at 540 cm^{-1} are the characteristic peaks for the spinel compounds) [30].

It is also understood that the presence of water of hydration in the spinel ferrites give rise to stability of the ferrite, which is understood from the infrared studies.

From application and instrumentation point of view, the infrared region has been subdivided into three parts.

- a) near infrared region 4290-400 cm^{-1} (0.7-2.5 μm);
- b) middle infrared region 4000-666 cm^{-1} (2.5-15 μm); and
- c) far-Infrared region 700-200 cm^{-1} (14.3-50 μm).

In the present investigation, the infrared spectra of nano articles were recorded on a Perkin-Elmer FTIR spectrophotometer [Model 1000] in the range 400 cm^{-1} to 4000 cm^{-1} .

- **Scanning Electron Microscopy (SEM)**

The shape, size and distribution of the grains of the powders, for the as prepared oxide samples, have been examined using a Leica-440 Cambridge Stereo scan, scanning electron microscope images. The SEM was operated at 20 kV. The samples were made conducting by the sputtering of gold using a 'Poloron DC sputtering unit' operated at 1.4 kV and 18-20 mA current. The SEM micrographs were taken using OR WO 35 mm film.

- **Transmission Electron Micrograph:**

The shape, size, nucleation and growth of grains can be observed by the as prepared oxide samples, have been examined using Technai-20 Philips for high resolution of nanoscopic images. The powdered sample was suspended in deionized water and the suspended particles are sonicated for 30 minutes, after sonication a drop of suspension was taken on a copper grid with carbon supported film. The sample was allowed to dry and then inserted for transmission scanning. The TEM was operated at 190 keV'.

- **Density Measurements:**

Tap Density:

The as-prepared voluminous oxide materials were hand crushed in agate mortar using a pestle and a known amount of this powder was filled into a graduated cylinder of 25 ml capacity. The cylinder was tapped until the powder level remains unchanged. The volume occupied by the powder was noted. The ratio between the weight of the substance and the volume gave tap density.

Powder Density:

The powder densities were measured using Archimedes principle [104-105] with a pycnometer and xylene as a liquid medium. The pycnometer of volume 25 ml was used. The following weights were taken and used in the density calculation.

$$\rho_{\text{sample}} = \frac{(W_2 - W_1)\rho_{\text{sol}}}{(W_4 - W_3) + (W_2 - W_1)}$$

Weight of the bottle	= W_1 g
Weight of the bottle + substance	= W_2 g
Weight of the bottle + substance + xylene	= W_3 g
Weight of the bottle + xylene	= W_4 g
Density of xylene	= ρ_{sol}
Density of sample	= ρ_{sample}

4. Result and Discussion:

• Fourier transform infrared spectroscopy (FT-IR) studies of CuO:

The Figure 1.1 the IR spectra of CuO metal oxide is shown in the respectively. The sample showed the absorption peaks at 3463, 1699, 1063, 1028, 849, 605, 502 cm^{-1} . The strong intense sharp peaks at 849, 605, 502 cm^{-1} are assigned to the metal oxygen vibrational mode. The peaks at 1063, 1028 cm^{-1} are due to the presence of some overtones.

The absorption bands observed in the region 3463 cm^{-1} and 1699 cm^{-1} in the sample is due to water of hydration.

• X-ray diffraction (XRD) studies of CuO:

The Figure 1.2 shows XRD pattern of the as synthesized CuO sample is indexed. The XRD pattern shows the formation of cubic phase of CuO. Unit cell parameters were obtained by least square refinement of the powder XRD data. The lattice parameters are in agreement with the data reported in literature (JCPDS 05-0661). The color of the above synthesized CuO is blackish blue.

• Energy dispersive microanalysis X-ray (EDAX) studies of CuO:

The EDAX spectra of as synthesized sample CuO are shown in Figure 1.3. This figure shows the presence of the Cu and O without any impurity signal in the sample.

• Scanning Electron Microscopy (SEM) studies of CuO:

Figure 1.4 SEM images of CuO shows agglomerated particle under low resolution they are interconnected each other under high resolution they separated each other.

• Elemental Analysis (C, H, N, S) of CuO:

The presence of Carbon, Hydrogen, Nitrogen and Sulphur (C, H, N and S) elements in CuO nanoparticles synthesized by using copper acetyl acetone was examined by elemental analysis as shown in table. From the above table it is clear that CuO consists of elements C & H. By this analysis along with elements we also come to know the percentage of these above mentioned elements. The percentage of carbon is 2.44 and hydrogen percentage is 0.96. But nitrogen and Sulphur is not detected in CuO nanoparticles.

• Transmission Electron Micrograph

Figure 1.5 shows the transmission electron micrograph of CuO particles, the morphology shows that the particles are agglomeration with dense interconnection. The shape of the CuO particle is bamboo shape structures and having sizes in between 50 to 100 μ m, this size and shape will enhance superior application comparing with the conventional method preparation.

- **Thermal Analysis:**

Figure 1.6. shows thermal analysis of CuO (copper(II) oxide) involves studying its behavior under different temperature conditions using techniques such as thermogravimetric analysis (TGA), differential scanning calorimetry (DSC), and differential thermal analysis (DTA). Here's a breakdown of key aspects:

a) Thermal Stability and Decomposition

- **Decomposition Temperature:** CuO is thermally stable up to approximately 900–1000°C in air.
- **Decomposition Reaction:** At higher temperatures (above 1015°C), CuO decomposes into Cu₂O (cuprous oxide) and O₂ gas:

$$4\text{CuO} \rightarrow 2\text{Cu}_2\text{O} + \text{O}_2 \quad (\text{above } 1015^\circ\text{C})$$
- Under reducing atmospheres (e.g., in hydrogen gas), CuO reduces to metallic copper at much lower temperatures (200–400°C).

b) Phase Transitions

- CuO has a monoclinic crystal structure at room temperature.
- No major phase transitions occur before decomposition under normal atmospheric conditions.
- In some cases, a metastable cubic phase can be observed at high pressures and temperatures.

c) Heat Capacity & Enthalpy

- The specific heat capacity (C_p) of CuO increases with temperature.
- Around 400-700°C, an endothermic peak is observed in DSC due to decomposition.

d) Applications of Thermal Analysis

- Used in designing ceramic materials, catalysts, and nanomaterials.
- Helps in understanding oxidation-reduction behavior in metallurgical processes.
- Important in battery and electronic applications where CuO is used in thermal coatings.

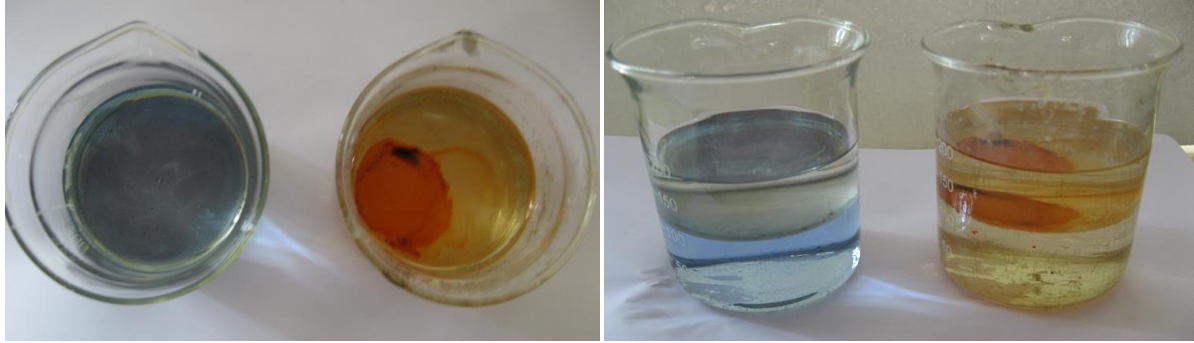


Figure 1. Shows interface reaction mixture of Copper acetyl acetonate

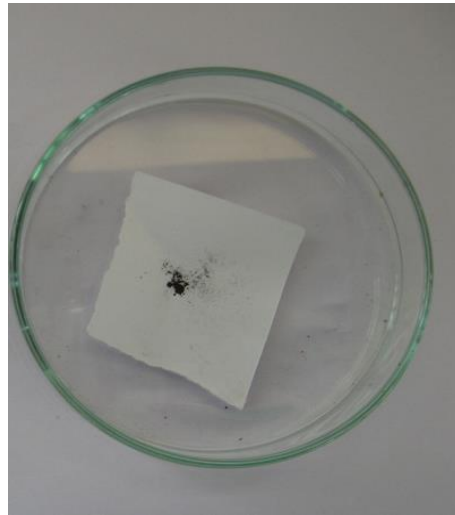


Figure 2. Shows the oxides of CuO

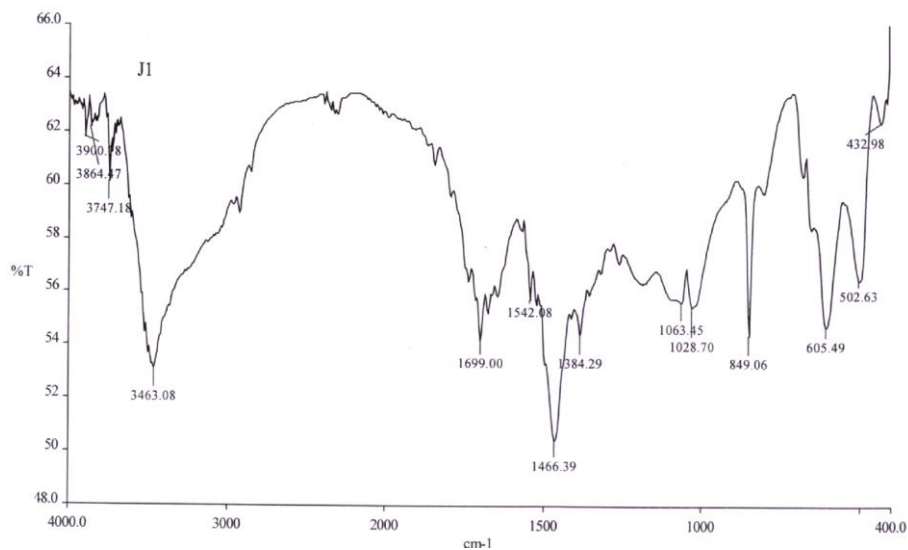


Figure 3. Shows IR spectra of as synthesized CuO nanoparticles

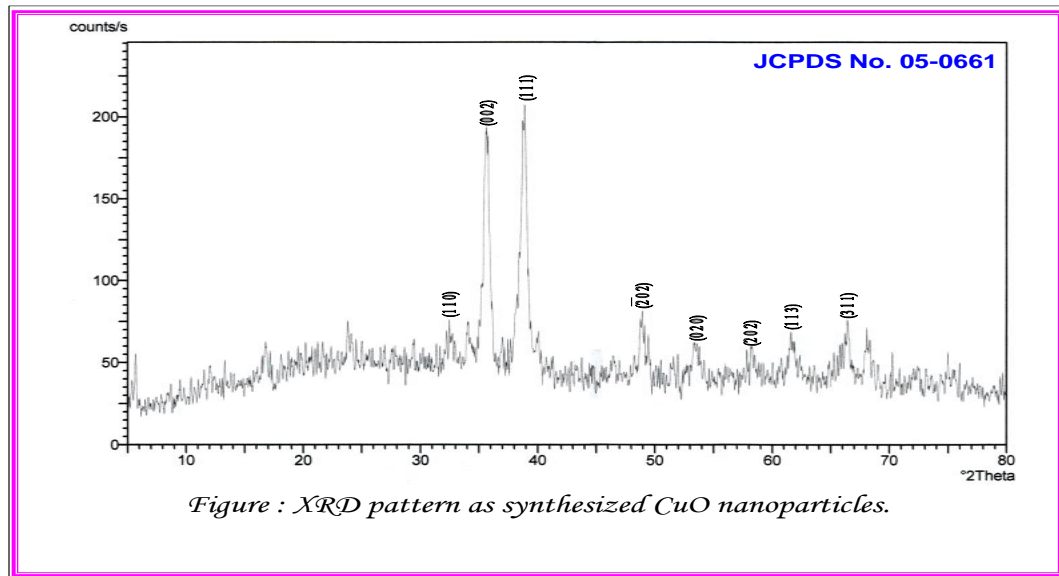


Figure 4. XRD pattern of as synthesized CuO nanoparticles

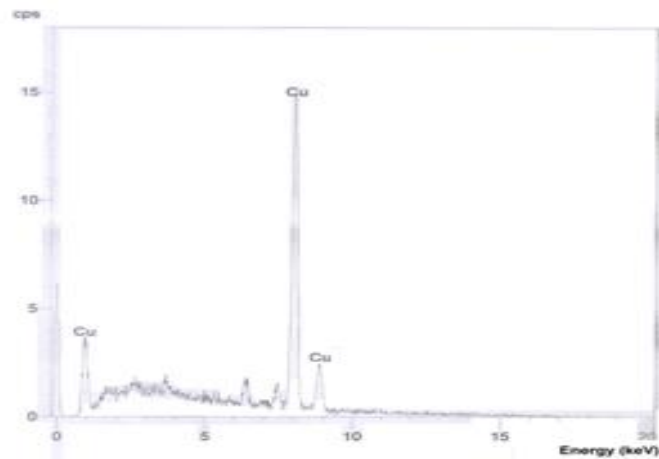


Figure 5. EDAX pattern of as synthesized CuO nanoparticles

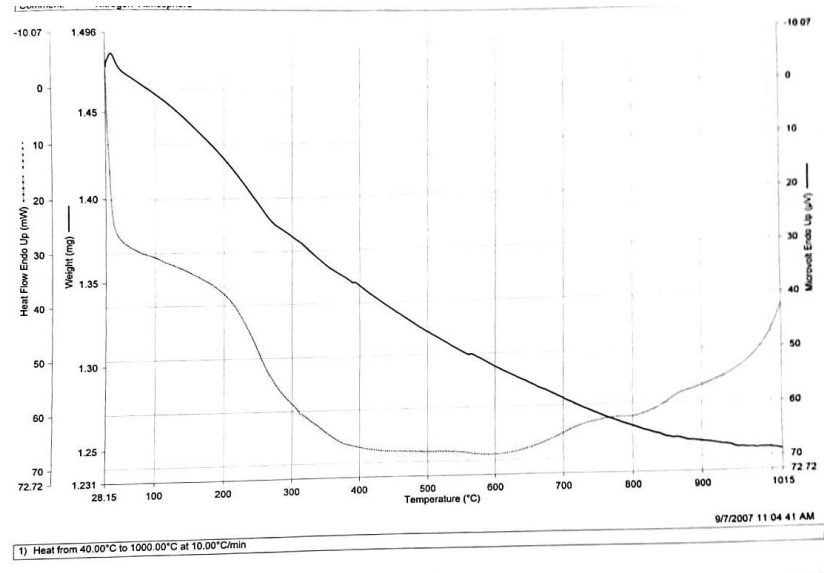
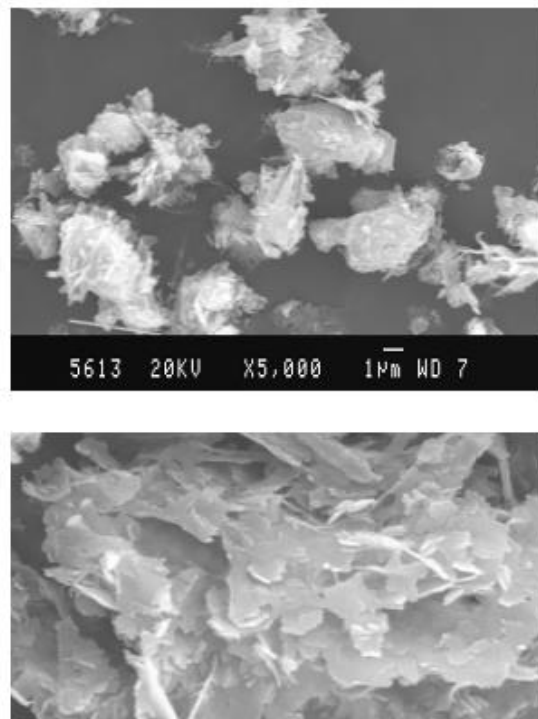


Figure 6. Thermal analysis of CuO nano-particles



SEM image of as synthesized CuO nanoparticles at (a) low and (b) high magnification.

Figure 7. SEM image of as synthesized CuO nanoparticles at (a) low and (b) high magnification

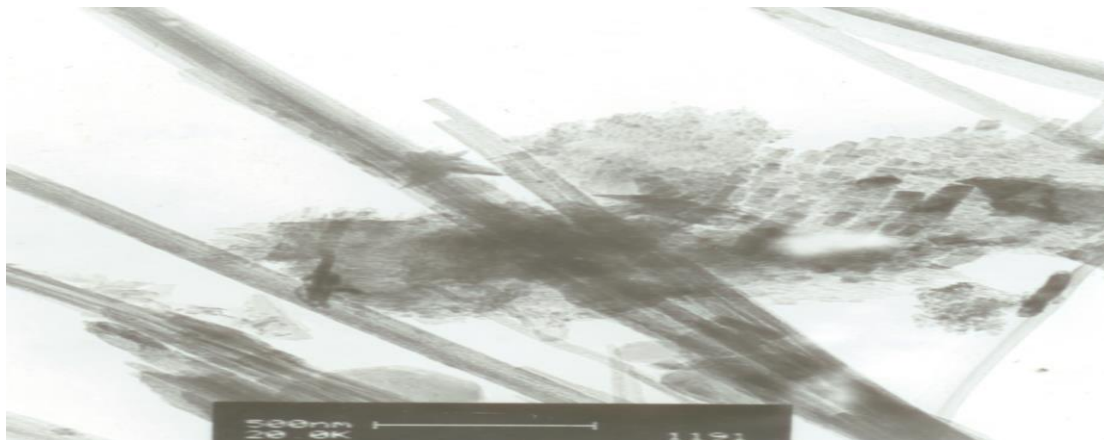


Figure: TEM image of CuO nanoparticles.

Figure 8. TEM image of CuO nanoparticles

Table 1. Elemental analysis and densities of synthesized metal oxides CuO

N%	ND	X-ray density (in Kg/m ³)	3728
C%	2.44	Tap density (in Kg/m ³)	4995
S%	ND	Bulk density (in Kg/m ³)	5030
H%	0.96		

5. Conclusion:

The experimental part includes the preparation of precursors of the respective metal complex which is dissolved in organic solvent and it is treated with alkaline medium (base), the reaction takes place at the interface and forms metal oxides consisting of nanosized particles. The characterizations of these metal oxides with IR, XRD, SEM and TEM give well authentic values with CuO. The thermal analysis gives strength and stability of the CuO. The method used for this is novel and advanced, low cost effective and high purity oxide are obtained.

Reference:

1. C.N.R. Rao, Chemical approaches to the synthesis of inorganic materials, Wiley Eastern Ltd., New Delhi (1994).
2. J. Livage, M. Henry and C. Sanchez, Prog. Solid State Chem. 18 (1988)259.
3. R. Schollhorn, In inclusion compounds, J. L. Atwood, J. Davis and MacNicol, Ed., Academic press London 1. (1984)249
4. J. Rouxel, In, International layered Materials, F.Lavi (Ed). Reidel Publishing, Dordrecht, Holland (1979)201.

5. L Babes, B. Denizot, G.Tanguy, J.J.L. Jeune and P. Jallet, *J. ColloidInterf. Sci.* 212(1999)474
6. P. K Gupta and C.T Hung, *Life Sci.* 44 (1999)175.
7. T. Fukushim, K. Sekizawa, Y. Jin, M. Yamaya, H. Sasaki and T. Takishima, *Amer. J. Physiol.* 265 (1993) L67.
8. Y. R. C Hemla, H. L. Groffman, Y. Poon, R. McDermott, R. Stevens and M. D. Alper, J. Clarke, *Proc. Natl. Acad. Sci* 97(2000).14268'
9. G. M. Whitesides, R. Kazlauskas and L. Joshephson, *Magnetic separation in Biotechnology, TIBTECH* 1 (1983) pp 144-148.
10. J. U. Ugelstad, A. Berge T. Ellingsen, R. Schmid, T.-N Milsen, P. C. Mork, P. Stenstad, E. Hornes and O. Olsvik, *Prog. Polym . Sci.* 17 (1992)87.
11. A. Jordon, R. Scholz, C. Wust, H. Schirra, T. S. chiestel, H. Schmidt, and R. Felix, *J. Magen, Magen. Mater.* 194(1999)185.
12. S. Liao, J. Zhu, W. Zhong, H. Y. Chen, *Mater.Lett.* 50 (2005)341.
13. A. Lagashetty V. Havanoor. S. Basawaraj, S. D. Balaji and A. Venkatraman, *Sci. Technol. Adv. Mater.* 8(2007)484.
14. J. Du and H. Liu, *J. M. agen, Magen. Mater.* 302 (2006)263.
15. J. Pinkas, V. Reichlova, R. Zboril, Z. Moravec, P. Bezdictka and J. Matejkova, *Ultrason. Sonochem.* 15 (2008) 257.
16. A. B. Chin and I. I. Yaacoob, *J. Mater. Process Technol.* 191 (2007) 235.
17. K. Woo, J. Hong, S. Choi, H-W. Lee, J-P. Ahn, C. S. Kim and S. W. Lee, *Chem. Mater.* 16 (2004) 2814.
18. T. Hyeon, S. S. Lee, J. Park, Y. Chung and H. B. Na, *J. Amer. Chem. Soc.* 123 (2001) 12798.
19. S. Chaianansutcharit, O. Mekasuwandumrong and P. Praserttham, *Cryst. Growth Des.* 6 (2006) 40.
20. Q. Guo, X. Teng, S. Rahman and H. Yang, *J. Amer. Chem. Soc.* 125 (2003) 630.
21. Y. Lin, H. Skaff, T. Emrick, A. D Dinsmore and T. P Russsekkm *Science* 299 (2003) 226
22. M. Brust, M. Walker ,D Bethell, D. J. Schiffrin and R. Whyman, *J. Chem. Soc. ChemCommun*, 7 (1994), 801
23. U. K Gautam . M. Ghosh and C., N. R Rao, *Langmuir* 20(2004) 10775
24. C. N. R. Rao Gu. U. Kulkarni, P. J Thomas, V. V. Agrwal. And P. Sarvanan, *J. Phys. Chem B* 107 (2003)7391
25. C. N. R Rao G. U. Kulkarni P. J. Thomas V. V. Agrwal, U. K. Gautam and M. Ghosh. *Curr.Sci* 85 (2003)104
26. C. N. R Rao G. U. Kulkarni, V.V. Agrawal. U.K Gautam. M Ghosh and T Tumkurkar, *J. Colloid Interf. Sci.* 289 (2005) 305
27. U.K. Gautam, M. Ghosh and C.N.R. Rao *Chem Phys. Lett.* 381 (2003)1.
28. A.R. West, "Solid State Chemistry and its Application" John Wiley New York (1989).
29. V.V.S.S Sai Sundar, Ph.D Thesis, Indian Institute of Science Bangalore 1995.

30. C.N.R. Rao, Chemical Approches to the Synthesis of Inorganic Materials, Weily Eastern Ltd, New Delhi (1994).